

1-1-1980

Radar Image Preprocessing

Victor S. Frost

Josephine A. Stiles

Julian C. Holtzman

D. N. Held

Follow this and additional works at: http://docs.lib.purdue.edu/lars_symp

Frost, Victor S.; Stiles, Josephine A.; Holtzman, Julian C.; and Held, D. N., "Radar Image Preprocessing" (1980). *LARS Symposia*. Paper 350.

http://docs.lib.purdue.edu/lars_symp/350

This document has been made available through Purdue e-Pubs, a service of the Purdue University Libraries. Please contact epubs@purdue.edu for additional information.

Reprinted from

**Symposium on
Machine Processing of
Remotely Sensed Data
and
Soil Information Systems
and
Remote Sensing and Soil Survey**

June 3-6, 1980

Proceedings

The Laboratory for Applications of Remote Sensing

Purdue University
West Lafayette
Indiana 47907 USA

IEEE Catalog No.
80CH1533-9 MPRSD

Copyright © 1980 IEEE
The Institute of Electrical and Electronics Engineers, Inc.

Copyright © 2004 IEEE. This material is provided with permission of the IEEE. Such permission of the IEEE does not in any way imply IEEE endorsement of any of the products or services of the Purdue Research Foundation/University. Internal or personal use of this material is permitted. However, permission to reprint/republish this material for advertising or promotional purposes or for creating new collective works for resale or redistribution must be obtained from the IEEE by writing to pubs-permissions@ieee.org.

By choosing to view this document, you agree to all provisions of the copyright laws protecting it.

RADAR IMAGE PREPROCESSING

VICTOR S. FROST, JOSEPHINE A. STILES,
JULIAN C. HOLTZMAN

Remote Sensing Laboratory, University of
Kansas

D. N. HELD

Jet Propulsion Laboratory

ABSTRACT

Standard image processing techniques are not applicable to radar images because of the coherent nature of the sensor. Therefore there is a need to develop preprocessing techniques for radar images which will then allow these standard methods to be applied. A random field model for radar image data is developed. This model describes the image data as the result of a multiplicative-convolved process. Standard techniques, those based on additive noise and homomorphic processing are not directly applicable to this class of sensor data. Therefore, a minimum mean square error (MMSE) filter was designed to treat this class of sensor data. The resulting filter was implemented in an adaptive format to account for changes in local statistics and edges. A radar image processing technique which provides the MMSE estimate inside homogeneous areas and tends to preserve edge structure was the result of this study. Digitally correlated SEASAT-A synthetic aperture radar (SAR) imagery was used to test the technique.

I. INTRODUCTION

The goal of spaceborne synthetic aperture radar (SAR) systems is to remotely collect information concerning agriculture, vegetation health, sea state, soil moisture, geology, snow-pack conditions, etc. This goal will be aided through manual and machine analysis of the SAR imagery. Manual interpretation may be required for geologic analysis while quantitative automatic processing will be needed for measuring soil moisture, agriculture, etc. In each case processing the image data is desirable to improve the quantity and quality of the extracted information. A random field model following [1] has been developed for radar data. This model accurately represents the noise process for radar image data as being convolved-multiplicative noise. Therefore, standard techniques developed for image processing in the presence of additive noise [2] or simple multiplicative noise which can be treated using homomorphic techniques [3]

are not directly applicable to SAR data.

The purpose of this paper is to present one digital processing algorithm which has been successfully applied to SEASAT-A SAR digital imagery. This technique was developed by first modeling the SAR system and data characteristics. Next a performance criterion was selected and an optimum filter designed with respect to it. Because of its mathematical tractability the minimum mean square error (MMSE) was used. This criteria had been applied with some success in the past to image processing of signal dependent noise [4,5]. the MMSE is not the only suitable performance criteria; others, for example those incorporating specific aspects of the human visual system [6], should be investigated in the future.

The following sections will present the system model used in this study and a summary of the development of the processing technique. An adaptive algorithm that changed its impulse response based on local statistics was the result of this theoretical analysis. This approach is similar to that followed by others [6,7,8], but here the criteria for adapting the impulse response is directly related to the specific form of the sensor data. That is, this technique has been specifically designed to treat radar image data. Results are presented next which illustrate the algorithm.

II. A SYSTEM MODEL FOR RADAR IMAGE PROCESSING

The spaceborne imaging radar is able to measure a quantity directly related to the terrain backscatter coefficient, σ^0 , as a function of position with relatively fine resolution (The SEASAT-A SAR had a spatial resolution of 25m as compared with 80m for LANDSAT). The terrain backscatter coefficient as a function of position will be defined as

$$\sigma^0(x,y). \quad (1)$$

This quantity will also be defined as being a deterministic function of position. The signal actually recorded is the random instantaneous terrain reflectivity which will be defined as

$$r''(x,y). \quad (2)$$

This quantity will be modeled as containing two random components. The first component represents the random changes in terrain backscatter across the scene. This comes about because a typical SAR scene is composed of many different target classes and thus field boundaries exist. The location of these field boundaries are not known a priori and thus are modeled as occurring randomly within the scene. In addition random variations arise from the changes in backscatter within individual fields. For example, wheat fields at the same time in the growing season and under similar physical conditions, e.g., the same soil moisture, are said to have a specific σ^0 . But SAR sensing a large wheat field will record slight variations (other than fading) due to changes in

backscatter across the field. Even though all wheat fields taken as an ensemble will exhibit an expected value defined as σ^0 , the SAR only senses one sample function of this ensemble. The component of the instantaneous terrain reflectivity which incorporates field boundaries and intra-field variations will be defined as $r'(x,y)$ and will be normalized by the resolution area of the sensor, A, i.e.

$$r(x,y) = \frac{r'(x,y)}{A} \quad (3)$$

Where $r(x,y)$ is the normalized $r'(x,y)$ and is a sample function of a random process with

$$\sigma^0(x,y) = E\{r(x,y)\} \quad (4)$$

where

$$\{r(x,y)\} = \text{ensemble of sample functions.}$$

As expected the random process $\{r(x,y)\}$ is not stationary in general. But if attention is focused on a homogeneous target area, A_T , then by definition $\{r(x,y)\}$ is stationary in A_T .

The second random component of the instantaneous terrain reflectivity is fading. Fading is a well-known phenomenon because it is observed whenever a coherent illumination is used [9,10]. If we define the instantaneous received power as $P_r|(x,y)$, i.e. received power given a position (x,y) , then the probability density function (for a Rayleigh target) across the ensemble of received power $\{P_r(x,y)\}$ at (x,y) is given by [9].

$$f_{P_r}(P_r|(x,y)) = [P_r|(x,y)]^{N-1} \exp\left[-\frac{P_r|(x,y)}{\bar{P}_r}\right] \frac{1}{(N-1)! \left[\frac{\bar{P}_r}{N}\right]^N} \quad (5)$$

where

$$\bar{P}_r = E[P_r|(x,y)]$$

N = Number of looks averaged

A simple change of variable yields [11]

$$P_r(x,y) = \frac{\bar{P}_r(x,y)n(x,y)}{2N} \quad (6)$$

where

$$\bar{P}_r(x,y) = E\{P_r(x,y)\}.$$

The random process $\{n(x,y)\}$ characterizes the fading variations [9]. Note that $n|(x,y)$ has a standard χ^2 probability density function and that

$$E\{n(x,y)\} = 2N = \bar{n} \quad (7)$$

$$\text{Var}\{n(x,y)\} = 4N = \sigma_n^2 \quad (8)$$

The process $\{n(x,y)\}$ is stationary. Next a relationship between the two components of the instantaneous terrain reflectivity will be defined. The expected return power $\bar{P}_r(x,y)$ is found from the radar equation [12] as

$$\bar{P}_r(x,y) = \frac{P_T G^2 \lambda^2 A \sigma^0(x,y)}{(4\pi)^3 R^4} \quad (9)$$

where

P_T = Transmitted power
 G = Antenna gain
 A = Resolution cell area
 R = Range distance to resolution cell

Using equation (4) \bar{P}_r can be written as

$$\bar{P}_r(x,y) = E\{r(x,y)\} \cdot K$$

where

$$K = \frac{P_T G^2 \lambda^2 A}{(4\pi)^3 R^4} \quad (10)$$

Applying equation (6)

$$P_r(x,y) = \frac{E\{r(x,y)\} \cdot n(x,y) \cdot K}{2N} \quad (11)$$

In practice though $E\{r(x,y)\}$ is not available only one sample function $r(x,y)$ is sensed by the radar so the actual received power (dropping the constants) is modeled as

$$P_r(x,y) = r(x,y) \cdot n(x,y) \quad (12)$$

The received power described above is not directly observable in most SAR systems because the antenna, receiver, correlator and film (or digital recorder) introduces a spatial correlation which can be described in total by a single point spread function, $h(x,y)$. Therefore the observed SAR image is modeled by

$$I'(x,y) = P_r(x,y) * h(x,y) = [r(x,y) \cdot n(x,y)] * h(x,y) \quad (13)$$

where

* denoted a convolution
 $I'(x,y)$ = observed SAR image

The dominant source of randomness in radar image data is fading. This model separates the stationary fading component, $n(x,y)$, from the backscatter component, $r(x,y)$. Once $r(x,y)$ is estimated, homogeneous areas will be easily found using standard image segmentation techniques. The following estimation technique attempts to remove the fading noise and thus generate an image of just $r(x,y)$.

Upon cursory examination of equation (13) it appears that deconvolution techniques could be applied to received power, $r(x,y) \cdot n(x,y)$, then homomorphic filtering used to estimate $r(x,y)$. Unfortunately radar image data has noise characteristics, i.e., small signal to noise ratios, which precludes the use of deconvolution techniques because those methods tend to amplify the

high spatial frequency noise.

III. SUMMARY OF THE ALGORITHM DEVELOPMENT

The minimum mean square error (MMSE) filter which will be derived next for radar image data is that linear transfer function, $m(t)$, which minimized ϵ^2 where

$$\epsilon^2 = E[(s(t) - m(t) * z(t))^2] \quad (14)$$

where

$t=(x,y)$, a point in the spatial plane
 $s(t)$ = desired signal
 $z(t)$ =observed signal

The transfer function $m(f)$ has been derived as [13]

$$M(f) = \frac{S_{zs}(f)}{S_z(f)} \quad (15)$$

where

$$M(f) = \int_{-\infty}^{\infty} m(t) e^{j2\pi ft} dt$$

$f=(f_x, f_y)$, a point in the spatial frequency plane
 $S_{zs}(f)$ =cross power spectral density
 $S_z(f)$ =power spectral density of z

Using the model derived above for the radar image data the MMSE filter for homogeneous (stationary) areas is found in general to be [14]

$$M(f) = \frac{S_{I_r}(f)}{S_I(f)} = \frac{\bar{n} S_r(f) H(f) - \bar{n} r^2 \delta(f)}{(S_r(f) * S_n(f)) |H(f)|^2 - (nr)^2 \delta(f)} \quad (16)$$

where

$$I(t) = I'(t) - E[I'(t)]$$

$$H(t) = \int_{-\infty}^{\infty} h(t) e^{j2\pi ft} dt$$

assuming that

$$H(f) = \text{rect}_B(f) \quad (17)$$

$$R_n(\tau) = \sigma_n^2 \delta(\tau) + \bar{n}^2 \quad (18)$$

$$R_r(\tau) = \sigma_r^2 e^{-a|\tau|} + r^2 \quad (19)$$

where B =system bandwidth

then the MMSE filter becomes the cascade of two filters, i.e.,

$$M(f) = [\text{rect}_B(f)] \cdot \left[\frac{K_1}{1 + 4\pi^2 \left(\frac{f}{\alpha}\right)^2} \right]$$

where

$$K_1 = \frac{2\bar{n}}{2n\sigma_r^2 + \sigma_n^2(r^2 + \sigma_r^2)} \quad (20)$$

The second term in this equation governs the major characteristics of the filter thus the impulse re-

sponse of the MMSE filter for radar image data can be written as

$$m'(t) = K_1 \alpha e^{-\alpha|t|} \quad (21)$$

where

$$\alpha = \sqrt{2a \left[\frac{\bar{n}}{\sigma_n} \right]^2 \left[\frac{1}{1 + \left(\frac{r}{\sigma_r}\right)^2} \right] + a}$$

The minimum mean square filter described by equation (21) has some interesting properties. We have tacitly assumed that both $\{r(t)\}$ and $\{n(t)\}$ are wide sense stationary random processes. This assumption regarding $n(t)$ is valid over an entire radar image because both n and σ_n^2 are functions of system parameters which can be assumed to be constant if the scene is composed of only Rayleigh targets. But $\{r(t)\}$ is stationary only in an individual homogeneous region and thus the filter is theoretically applicable in only those areas. We will next show that even though this filter is theoretically valid for homogeneous regions if α is varied (adapted) with respect to scene conditions then the filter does not overly degrade edges between homogeneous areas. Similar techniques have been successful [1,8].

Consider two homogeneous (stationary) areas A_1 and A_2 with $r_1=r_2$ and $\sigma_{r_1}^2 < \sigma_{r_2}^2$ then from the equation (21) we find that

$$\alpha_1 > \alpha_2 \quad (22)$$

This result indicates that the impulse response of the MMSE filter for A_1 is narrower than the filter for A_2 . Because $\{r(t)\}$ is the quantity being estimated this is expected, i.e., if $r(t)$ has a large variance then a wide impulse response would excessively average the desired variation in backscatter; thus for areas with σ_r^2 large the impulse response of the filter should be narrow. On the other hand if $r(t)$ has a small variance then a wide impulse response would be advantageous.

Next consider an area, A_3 , which contains a boundary between two stationary areas A_1, A_2 . First note that A_3 is not a stationary area so theoretically this filter does not provide the minimum mean square estimate. But let us investigate its properties at an edge to evaluate its practical application to real radar image data. The presence of an edge will result in a large variance (i.e. bandwidth) for $r(t)$ in A_3 . We would thus expect

$$\sigma_{r_3}^2 > \sigma_{r_1}^2 \quad (23)$$

$$\sigma_{r_3}^2 > \sigma_{r_2}^2 \quad (24)$$

So for an area encompassing an edge this MMSE filter will average less and therefore preserve edge structure.

If α is estimated from the observed data within some neighborhood the filter would then adapt

to local changes in \bar{r} and σ_r^2 . This type of estimation technique would then exhibit two very important characteristics. First it provides the minimum mean square estimate of $r(t)$ in homogeneous areas. Second it tends to preserve edge structure.

As mentioned above α must be estimated from the observed data so that the filter will exhibit the desired properties. It can be shown that [14]

$$\alpha = K_2 \left[\frac{\sigma_{I'}^2}{\bar{I}'} \right]^2 \quad (25)$$

where

K_2 = constant of proportionality

$\sigma_{I'}^2$ = observed image variance

\bar{I}' = observed image mean

Therefore we estimate $\left(\frac{\sigma_{I'}^2}{\bar{I}'} \right)^2$ in local regions (e.g. a 5x5 neighborhood) and α adaptively change in proportion to $\left(\frac{\sigma_{I'}^2}{\bar{I}'} \right)^2$ as the impulse response is applied to the radar image. The resulting technique is the MMSE estimate within homogeneous areas and tends to preserve edge structure.

IV. RESULTS

An adaptive algorithm as described in the previous section was implemented. The program requires three parameters. The first parameter defines the number of different filters, NF , to be used. That is, the program calculates $\left(\frac{\sigma_{I'}^2}{\bar{I}'} \right)^2$ for a local region then uses that value to select one of NF precalculated weightings. Even though all examples presented here used a neighborhood (observation area to calculate $\left(\frac{\sigma_{I'}^2}{\bar{I}'} \right)^2$ and a filter size of 5x5 pixels, the program is designed to accept different neighborhoods and filter sizes. The next parameter required is directly proportional to the constant K_2 in equation (25). A maximum α , α_m , is specified and each filter is calculated using

$$m(x,y) = e^{-x \left(\frac{i+1}{s} \right)} e^{-y \left(\frac{i-1}{s} \right)} / \eta \quad (26)$$

where

i = filter number

$s = NF - 2 / \alpha_m$

η = normalization factor

The first filter ($i=1$) uses equal weighting for all elements and the last filter ($i=NF$) uses unity weighting on the center element and zero weighting on all others. The second through $NF-1$ filters are defined by equation (26). The final parameter used in this algorithm defines how the measured local statistics are used to select a particular filter. A constant K_3 is selected and the i^{th} filter is chosen by

$$i = K_3 \left(\frac{\sigma_{I'}^2}{\bar{I}'} \right)^2 \quad (27)$$

To summarize the procedure, first the three parameters, NF , α_m , and K_1 are specified. Next, the algorithm precalculates $NF-2$ filters (remember the first and last filters are fixed) using α_m . Third, a moving window of variable size is used to gather local statistics $\left(\frac{\sigma_{I'}^2}{\bar{I}'} \right)^2$ around each pixel and this information is used to select a specific filter. The final step involved applying the filter to the original radar image data. The results presented here used $NF=40$, $\alpha_m=6.5$, $K_3=75$.

The first scene used was a test area which contained a series of corner reflectors. These are point targets in the resulting SEASAT-A SAR imagery. This processing algorithm was applied and in the resulting image the point targets remained basically unchanged while the noise was significantly reduced in homogeneous areas (Figure 1). The second scene was near Knoxville, Tenn., and contained significant terrain relief. The processed SAR image of this area shows how the technique improved the utility of spaceborne SAR data for geologic interpretation (Figure 2). The final area contained several agricultural fields (Figure 3).

V. CONCLUSION

A systems model for an imaging radar has been developed and used to design an image processing technique which has been successfully applied to processing SEASAT-A SAR imagery. Results have been presented which show the utility of this technique. A quantitative evaluation of the results is currently under way. But the problems associated with radar image processing have just begun to be addressed. Refinements in the optimization criteria are required. Better systems modeling, i.e., an accurate representation of $h(t)$ would also improve the techniques. Investigations of feature classification from radar data are also necessary.

ACKNOWLEDGMENTS

This work was supported by the California Institute of Technology President's Fund and NASA Contract NAS 7-100 and the Army Research Office Contract DAAG29-77-6-0075.

REFERENCES

- [1] Rosenfeld, A. and L.S. Davis, "Image Segmentation and Image Modeling," Proceedings of the IEEE, Vol. 67, No. 5, May 1979.
- [2] Pratt, W.K., "Digital Image Processing," John Wiley and Sons, New York, 1978.
- [3] Oppenheim, A.V., R.W. Schaffer, and T.G. Stockham, "Nonlinear Processing of Multiplied and Convolved Signals," Proceedings of IEEE Vol. 56, No. 8, 1968.

- [4] Kondo, K., Y. Ichioka, T. Suzuki, "Image Restoration by Wiener Filtering in the Presence of Signal Dependent Noise," Applied Optics, Vol. 16, No. 9, Sept 1977
- [5] Walkup, J.F., R. C. Choens, "Image Processing in Signal Dependent Noise," Optical Engineering, May/June 1974.
- [6] Pearlman, W.A., "A Visual System Model and a New Distortion Measure in the Context of Image Processing," J. Opt. Soc. Am. Vol. 68, No. 3, March 1978.
- [7] Panda, D.P., "Nonlinear Smoothing of Pictures," Computer Graphics and Image Processing, Vol. 8, pp. 259-270.
- [8] Chen, C.H., "Adaptive Image Filtering," Proc. Pattern Recognition and Image Processing, Chicago, Ill., Aug. 1979.
- [9] Bush, T.F. and F. T. Ulaby, "Fading Characteristics of Panchromatic Radar Backscatter from Selected Agricultural Targets," IEEE Trans. Geoscience Electronics, Vol. 6E-13, Oct. 1976.
- [10] Goodman, J.W., "Some Fundamental Properties of Speckle," J. Opt. Soc. Am, Vol. 66, No. 11, Nov, 1976.
- [11] Frost, V.S., "Development of Statistical Models for Radar Image Analysis and Simulation," Master of Science Thesis, The University of Kansas, 1978.
- [12] Reeves, R.G., A. Anson, D. Landen, "Manual of Remote Sensing," Vol 1, Chapter 9, American Society of Photogrametry, Falls Church, Va. 1975.
- [13] Davenport, W.B., and W. L. Root, "Random Signals and Noise," McGraw-Hill Book Co., New York 1958.
- [14] Frost, V. S., J.A. Stiles, J.C. Holtzman, "Radar Image Processing," Technical Report TR 420-1 Remote Sensing Laboratory, The University of Kansas, Jan., 1980.

Original



Processed



Figure 1
SEASAT-A SAR Image (1 Look) Point Targets

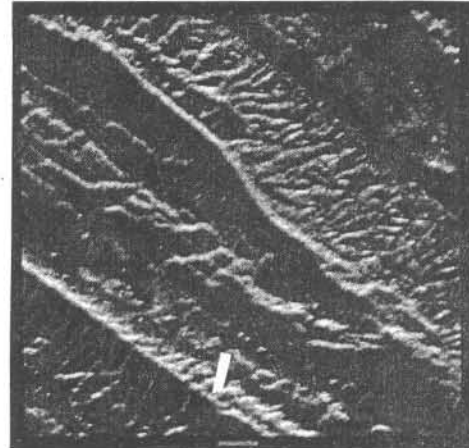
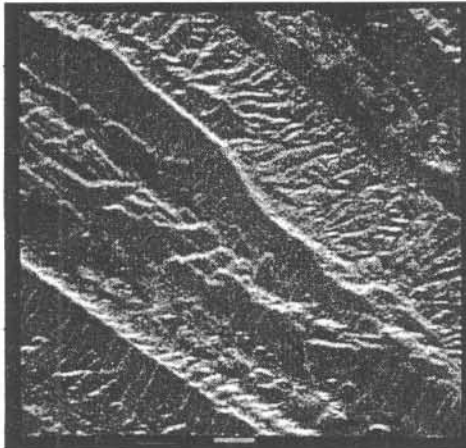


Figure 2
SEASAT-A SAR Image (4 Looks) Geologic Features

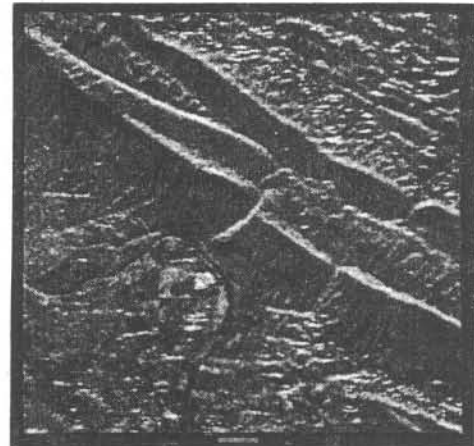
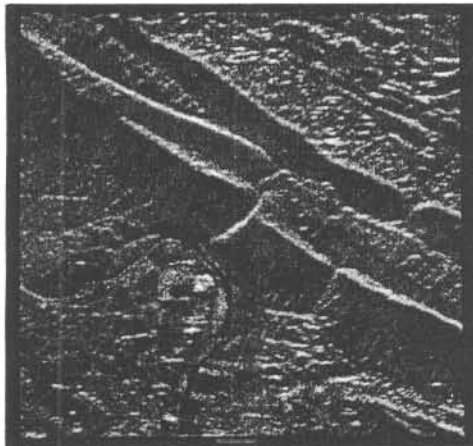


Figure 3
SEASAT-A SAR Image (4 Looks) Agricultural Features